EFFECT OF HYDROGEN ON DEFORMATION STRUCTURE AND PROPERTIES OF CMSX-2 NICKEL-BASE SINGLE-CRYSTAL SUPERALLOY

M. Dollar, I.M. Bernstein, S. Walston,
F. Prinz, and A. Domnanovich
Carnegie Mellon University
Pittsburgh, Pennsylvania

Material used in this study was a heat of the alloy CMSX-2 whose chemical composition is given in Table I. This nickel-based superalloy was provided in the form of [001] oriented single crystals, solutionized for 3 hrs at *1315*°C. It was then usually heat treated as follows: *1050*°C/16h/air cool + *850*°C/48h/air cool. The resulting microstructure is dominated by cuboidal, ordered γ' precipitates with a volume fraction of about 75% and an average size of 0.5 μm (Figure 1).

In previous studies (1,2) of hydrogen effects in the alloy we have shown that a high hydrogen fugacity environment can degrade room temperature mechanical properties. Hydrogen was introduced by cathodic potentiostatic charging in a mixture of two molten salts, 57% sodium bisulfate and 43% potassium bisulfate at *150*°C for 5 hrs. The most significant effects of such charging were on tensile behavior, where a 34% loss of homogeneous elongation was found and on push-pull fatigue behavior where a several-fold decrease of the accumulated plastic strain to fracture resulted, over a wide plastic strain range down to 0.02%. A detailed microscopic interpretation of these hydrogen-induced effects was limited by the fact that the hydrogen introduced by the molten salt charging resided primarily in a surface layer about 50 μm in depth.

To better understand and control the role of hydrogen, high pressure, high temperature hydrogen charging was carried out at Sandia National Laboratory-Livermore, CA. This entailed gas phase charging for 15 days at *300*°C under a pressure of 138MPa, and furnace cooling to room temperature in 16 hrs. under pressure. A resultant, uniform hydrogen concentration of the order of 5000 appm across the entire cross-section of 3 mm thick samples was obtained by such a procedure.

As shown in Tables II and III, and in Figure 2, this charging mode more dramatically changes tensile and fatigue behavior than molten salt charging. The presence of this significant amount of dissolved hydrogen, while not significantly changing the relatively high yield strength, does promote significant work hardening, in contrast to hydrogen-free material where softening is found, and also dramatically reduces the true uniform elongation to almost zero. In fatigue, the number of cycles to failure now drops two order of magnitude and the occurrence of strain localization is more pronounced then in either the hydrogen-free case, or when the hydrogen was localized at the surface.

TEM and SEM evidence provides a picture of how hydrogen can affect the deformation structure and the fracture of CMSX-2 and can be used to correlate changes in mechanical properties with the presence of hydrogen in both the γ and γ' phases. In brief, the most compelling hydrogen induced-changes in deformation structure are : i) enhanced dislocation accumulation in the γ matrix; and ii) more extensive cross-slip of superdislocations in the γ' precipitates. These are shown in Figures 3 and 4, respectively (for comparison see also Figures 5 and 6 which illustrate the deformation structure of H-free material). The enhanced dislocation density in γ acts to decrease the mean free path of a superdislocation, while easier cross slip hinders superdislocation movement by providing pinning points in the form of sessile jobs. Both processes contribute to the increase of flow stress and the notable work hardening that occurs prior to fracture.

Previously (1,2), examination of fractured tensile samples revealed that uncharged samples fractured predominantly along planes parallel to multiple, crystallographic {111} slip systems. The fractured surface was jagged and significant localized and general ductility was observed. In the present study, the hydrogen-charged samples were found to be much more brittle in appearance with a fracture surface that was quite planar and oriented normal to the tensile axis. A most striking SEM observation was that microcracks appear to follow <001> oriented γ/γ' interfaces (Figure 7) suggesting that preferrential cracking parallel to {001} planes occurs. However, TEM observations strongly suggests that a difference exists in the macroscopic and microscopic nature of hydrogen-induced crack initiation and propagation. In particular, Figure 8 clearly shows that cracking is associated with processes in the γ, manifested as localized tearing in thin foils. While at first sight these appear to follow {001} planes, in reality they are comprised of short segments on multiple {111} planes. While tearing in thin foils is clearly not identical with microcracking in bulk material, it is suggestive and we believe accurately so, that embrittlement results from hydrogen-enhanced strain localization, resulting in dislocation intensification in the narrow ribbons of γ and premature plastic failure due to strain exhaustion and the apparent mode I fracture.

This work is being supported by NASA-Lewis under the technical direction of Dr. Robert Dreshfield.

References

1. Bernstein, I.M., et al.: Proceedings of the 1986 NASA Conference on Advanced Earth-to-Orbit Propulsion Technology, May 1986.

2. Baker, C.L., et al.: to be published in Metall. Trans., 1987

TABLE I

CMSX-2 Composition (wt. %)

Cr	8.0
W	8.0
Ta	6.0
Al	5.6
Co	4.6
Ti	1.07
Mo	0.6
Fe	0.08
Si	0.015
Ni	balance
C	15 ppm
S	10 ppm
N	4 ppm
O	2 ppm

TABLE II

Tensile Behavior as a Function of Charging Condition

Charging Conditions	YS (MPa) (0.2% offset)	UTS (MPa)	Homogeneous Elongation (%)	Elongation Loss (%)
uncharged	917	987	21.7	---
molten salt 5h at 150°C	856	976	14.4	33.6
gas phase 5 days at 138MPa & 300°C	935	1123	1.2	94.5

TABLE III

Fatigue Behavior as a Function of Plastic Strain Range and Charging Conditions

$\Delta\epsilon_p$(%)	Charging Conditions	Cycles to Failure uncharged	charged	n_u/n_c	Accum. Plastic Strain ($n \times \Delta\epsilon_p$) (%) uncharged	charged
0.4	molten salt 5h at 150°C	57	16	3.6	46	13
0.2		131	57	2.3	52	23
0.1		214	80	2.7	43	16
0.02		3348	1260	2.7	137	53
0.02	gas phase 15 days at 138MPa & 300°C	6664	21	317	267	.84
0.02		3085	16	193	123	.56
0.02		2483	29	86	99	1.16

R = −1, Room Temperature Testing

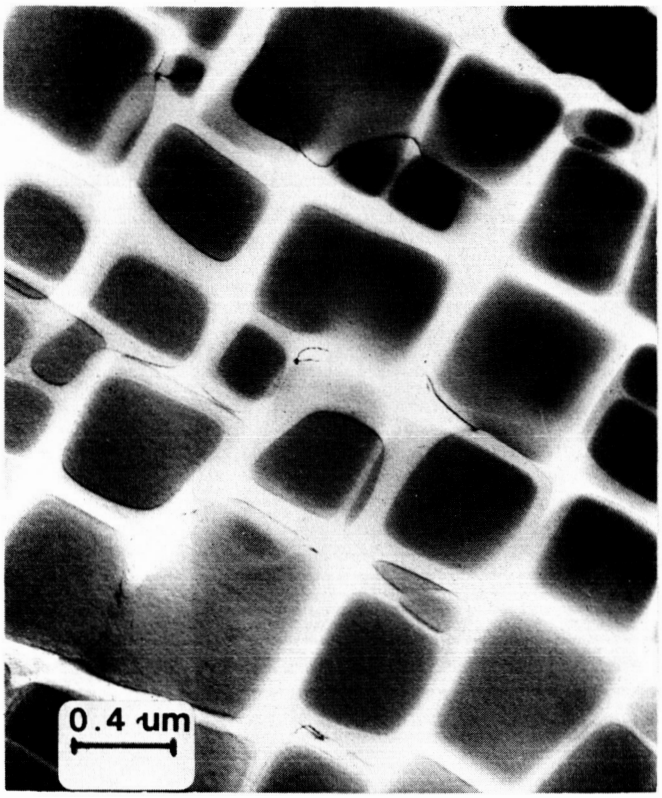

ORIGINAL PAGE IS
OF POOR QUALITY

Figure 1. - TEM micrograph, initial microstructure of CMSX-2.

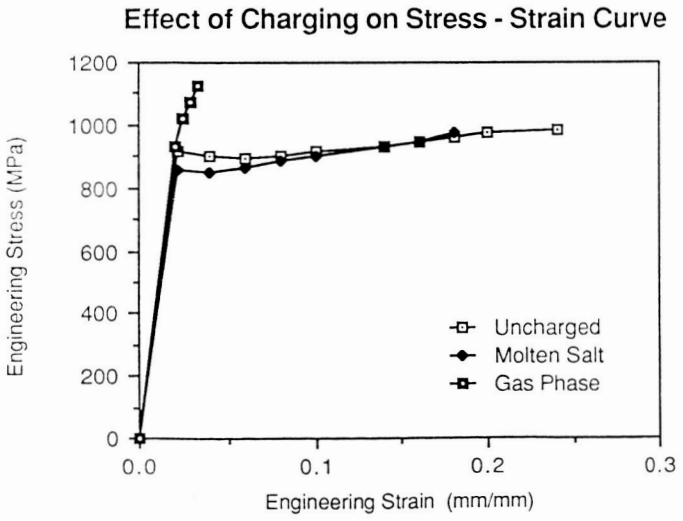

Figure 2. - Influence of hydrogen charging on tensile behavior of CMSX-2.

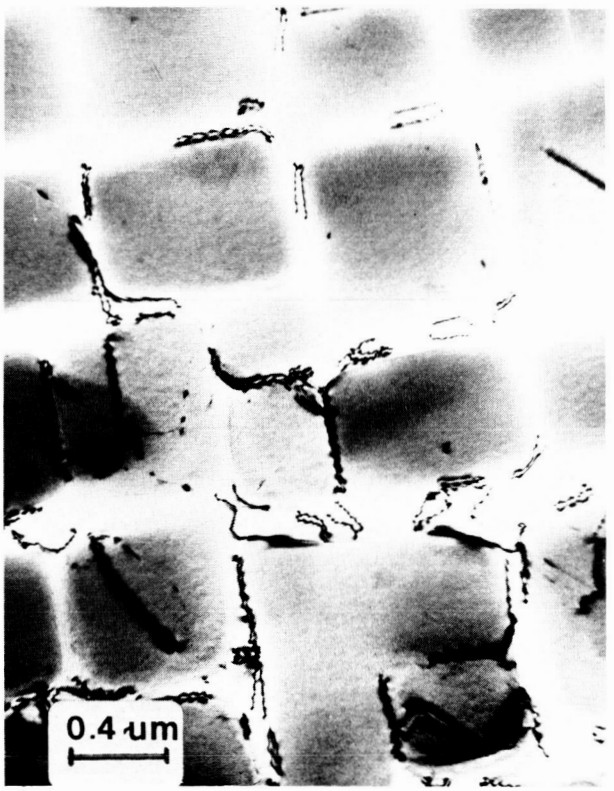

Figure 3. - Typical deformation structure of hydrogen-charged CMSX-2; ε = 0.8 percent.

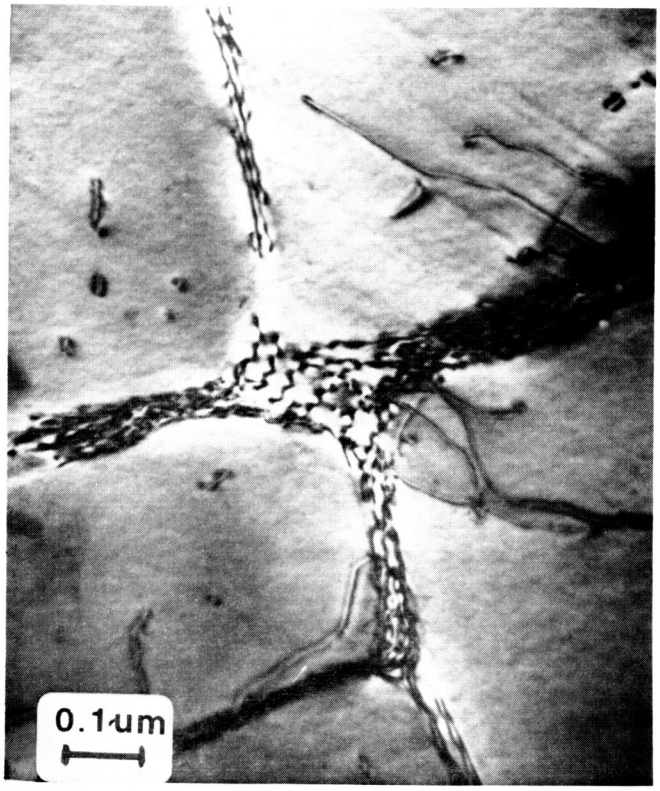

Figure 4. - Typical deformation structure of hydrogen-charged CMSX-2; ε = 1.2 percent.

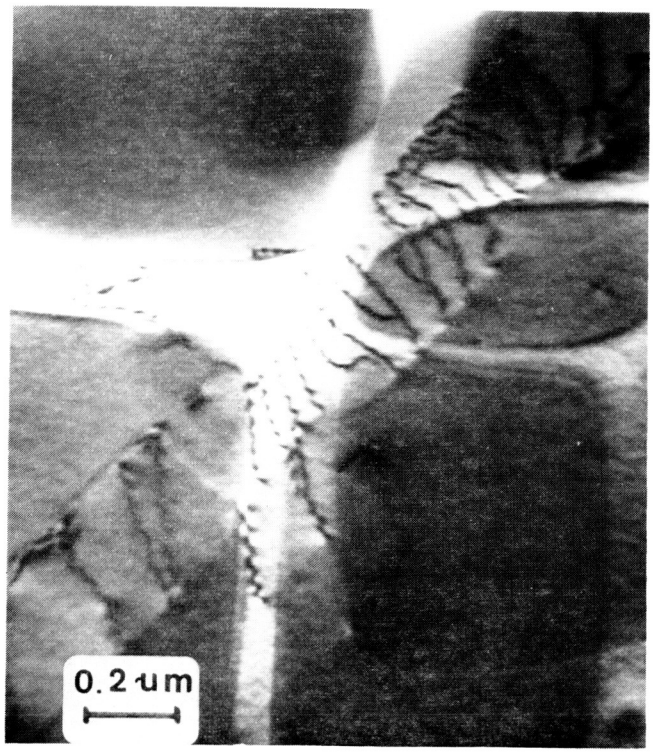

Figure 5. - Typical deformation structure of hydrogen-free CMSX-2; ε = 4 percent.

Figure 6. - Typical deformation structure of hydrogen-free CMSX-2; ε = 5 percent; (foil cut parallel to (111) slip plane).

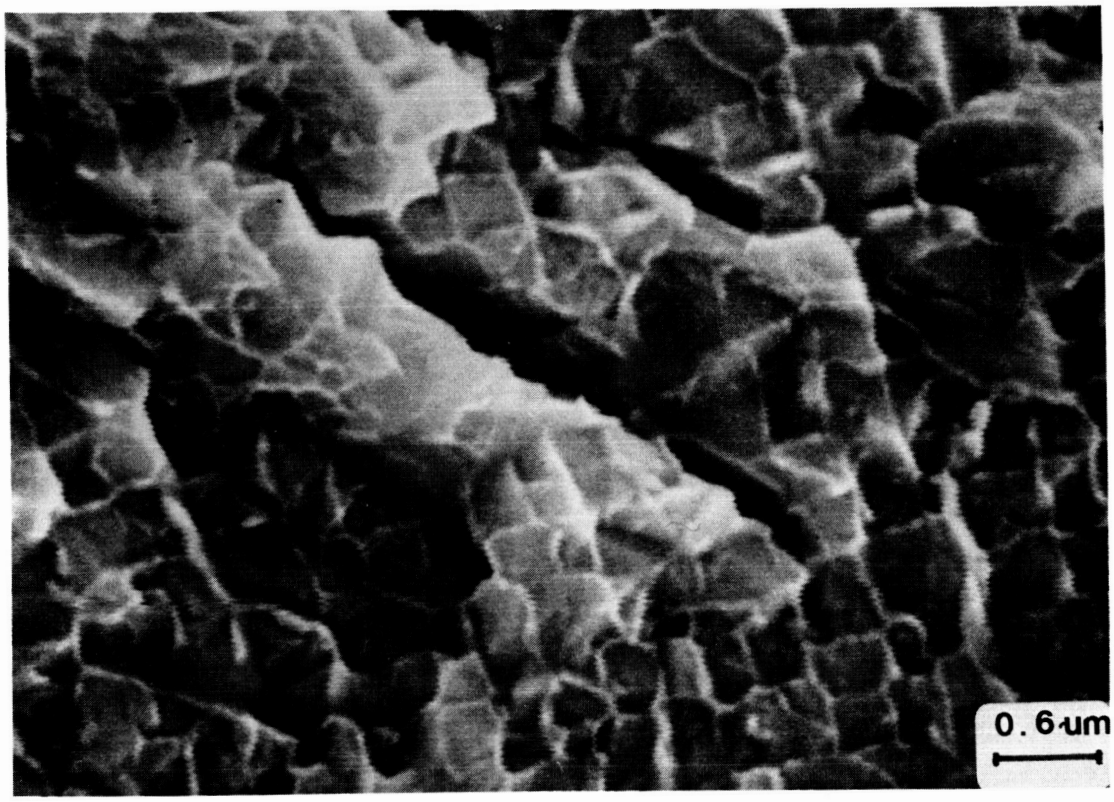

Figure 7. - Fracture surface of hydrogen-charged CMSX-2.

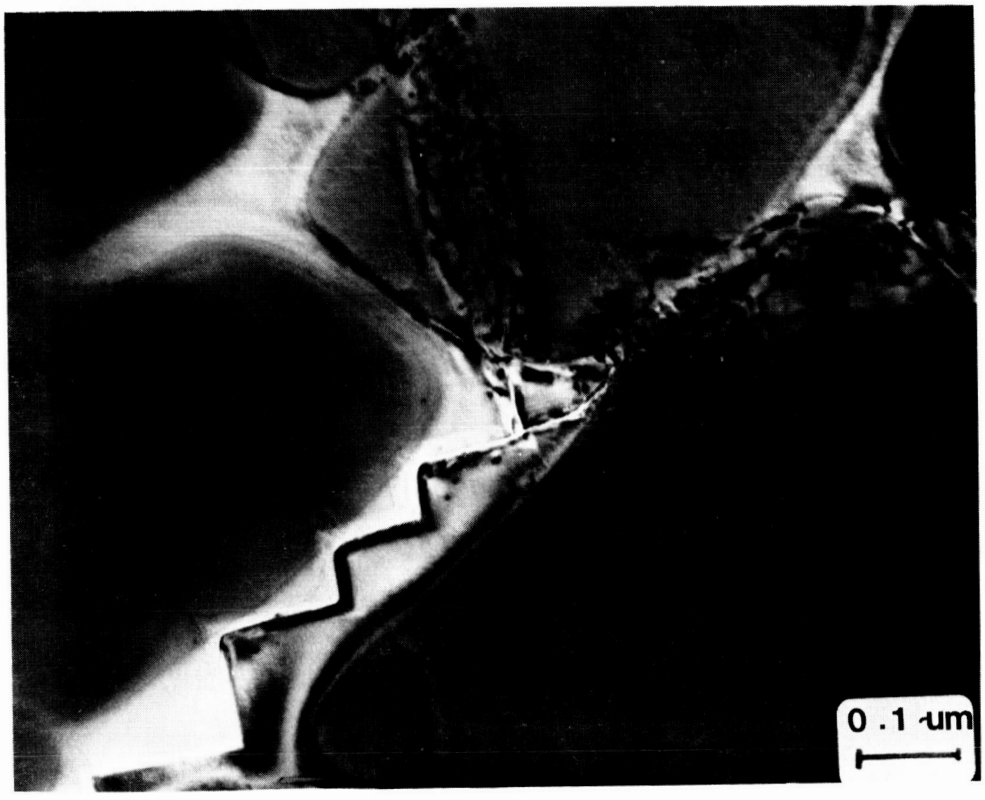

Figure 8. - Tearing in a thin foil cut close to fracture surface. (Material was hydrogen-charged.)